ISSN 1064-2293, Eurasian Soil Science, 2020, Vol. 53, No. 3, pp. 267–282. © Pleiades Publishing, Ltd., 2020.
Russian Text © The Author(s), 2020, published in Pochvovedenie, 2020, No. 3, pp. 261–278.

GENESIS AND GEOGRAPHY OF SOILS

# Reconstruction of the Climate of the Medieval Epoch Based on Soil and Geochemical Studies of Kurgans of the Srostki Culture in the South of Western Siberia[1]

**V. E. Prikhodko[a, *], Yu. A. Azarenko[b], M. R. Shayakhmetov[b], A. A. Tishkin[c], V. V. Gorbunov[c], and E. G. Pivovarova[d]**

[a] *Institute of Physicochemical and Biological Problems in Soil Science, Russian Academy of Sciences, Pushchino, 142290 Russia*
[b] *Stolypin Omsk State Agrarian University, Omsk, 644008 Russia*
[c] *Altai State University, Barnaul, 659049 Russia*
[d] *Altai State Agrarian University, Barnaul, 656049 Russia*
**e-mail: valprikhodko@rambler.ru*

Received May 23, 2019; revised October 16, 2019; accepted October 30, 2019

**Abstract**—The environmental diversity of Altai region is of great interest for researchers. There are many monuments of cultural heritage in the region, which are still poorly studied by natural scientific methods. Paleosols and background soils of the large Srostki-I necropolis of the Early Medieval epoch was examined by pedological and geochemical methods with the aim to trace changes in the soil properties over time and to apply these data for reconstruction of the paleoclimate. This group of kurgans is located in Biysk district of the Altai region and, according to the radiocarbon method, dates back to 890 ± 105 – 975 ± 85 AD (calibration 1δ). Paleosols of the Medieval epoch are characterized by a weaker leaching of carbonates in the middle part of the profile, lower accumulation of biophilous elements (P, S, Co) in the upper horizons, and lower values of the weathering index $Al_2O_3/(CaO + MgO + Na_2O + K_2O)$ in comparison with the background surface soils. Thus, in the period before the kurgans' construction, these paleosols were formed under somewhat drier climate in comparison with the present time. However, the similarity of these paleosols and background surface soils in their morphological properties, reconstructed humus content, and averaged values of weathering indices $Al_2O_3 \cdot 100/(CaO + MgO + Na_2O + K_2O)$ and Rb/Sr, as well as Mn/Sr, Mn/Al, and Mn/Fe indices characterizing the degree of biological activity attest to humidization of the paleoclimate during the period of construction of the kurgans. Among highly hazardous pollutants of the first toxicity class, the studied soils are enriched with As and Cd (in comparison with natural abundances of these elements in the lithosphere). In general, regional soils and parent material are enriched with As, Ni, Zn, Ba, and Sn, though the concentrations of these heavy metals in the soil profiles remain below the corresponding maximum permissible concentrations. The accumulation of toxic substances under the impact of anthropogenic pollution in the profiles of studied soils does not exceed the permissible values. The concentrations of heavy metals in the background surface soils are no higher than those in the medieval paleosols. The application of GIS technology demonstrated that 21 settlements and 130 necropolises of the Srostki community (second half of the 8th–12th centuries AD) were localized on fertile soils of leveled areas near large lakes and rivers (the Ob, Katun, Biya, Alei, and other rivers) and within wide valleys at the confluence of small streams with larger water bodies.

*Keywords:* paleoclimate reconstruction, paleosol, geochemical coefficients, pollutants, GIS technology, Altai region

**DOI:** 10.1134/S1064229320030059

## INTRODUCTION

The Altai region has been occupied by humans since the ancient time. There are several famous archaeological sites in this region: the oldest Karama site (Early Paleolithic period); world-famous monument of Denisova Cave, where people belonging to a separate branch of the evolution of the genus *Homo* lived since 280 ka BP [57]; the unique Pazyryk kurgans, where mummies with tattoos, carpets, clothes, jewelry, etc. were preserved thanks to the permafrost formed in the graves [30]. A large Early Medieval burial site Srostki-I is famous as well [8, 38]. Archeologists have studied hundreds of monuments of different time intervals of the Holocene, and thousands of kurgans in the south of Western Siberia and in the

[1] The article contains additional materials available for authorized users on doi: 10.1134/S1064229320030059

Altai Mountains. However, only a few of them were studied by the methods of natural sciences, including paleoclimate reconstruction. It is especially important to know the parameters of climate change over the last 2000 years in order to give a more accurate forecast of its dynamics in the future.

The soil cover, like other natural archives, can serve as a record preserving information (memory) about current and past environmental conditions [2, 10, 15, 22, 23, 31, 39, 45, 60, 63, 69]. For plains of the Altai region, there are few detailed reconstructions of the Holocene evolution of the environment. For mountainous area of the Altai region, information on paleoecosystems and paleoclimate was obtained based on the study of buried soils [5, 11, 46].

For example, a morphogenetic study of buried Holocene soils was performed for several profiles in the southeastern Altai Mountains that currently are formed in an arid climate. It was demonstrated that the conditions of soil formation during the last 1–2 ka were the most extreme throughout the entire Holocene [46]. The reconstruction of the natural conditions of the Holocene was based on the study of boundaries and sizes of glaciers, the water level of lakes, dendrochronology, and paleosol characteristics in the high mountains of southeastern and southern Altai. These studies demonstrated that in 884–1110 AD ($^{14}$C cal.) mountain glaciers receded noticeably, the tree line was located higher than it is today, and the air temperature of summer months was higher by 0.4 °C than it is today. Radiocarbon dating (54 $^{14}$C dates, including AMS dates) was performed for the remains of the trees found in the area of modern glaciation at 2400 m a.s.l. [41].

The studies of humus content and palynology of paleosols and sediments at the neighboring territories of the Tuva Republic showed a general trend of climate changes in the Holocene was directed towards cooling and aridization along with temperature and humidity fluctuations in different time intervals. Steppe landscapes were formed at the stages of increasing heat supply, while forest-steppe and taiga landscapes were developed during the stages of cooling. During the Subatlantic period, humid conditions were dominant at its beginning and arid conditions prevailed in the middle and at the end of this period; warm phases corresponded to the beginning (Subatlantic 1) and end (Subatlantic 3) of this period, and cold phase was established in the middle. A study of cutan assemblage and radiocarbon dating of soils in the mountainous southwestern part of Tuva region showed that the climatic conditions in the medieval epoch were close to those at present [5]. A comprehensive study of several paleosols on alluvial sediments formed over the last 13 thousand years in the intermontane arid basin near Lake Terekhol in the Sayany Mountains led to a conclusion about the most continental and arid climate over the last 2000 years [45].

In the adjacent region—forest-steppe zone of Novosibirsk oblast—the study of soils buried under the kurgans demonstrated that the climate in the 11th–13th centuries AD was favorable for dwelling of people [29].

Spore-pollen data obtained from sediments of lakes, rivers, and bogs are the most studied record of the climate and landscapes of the Holocene; their study is often accompanied by a set of other analyzes. Reconstruction of the climate in different periods of the Holocene was performed on the basis of palynological and landscape studies in the Altai region [24, 26, 27, 32, 42, 53, 77, 78]. A compilation of palynological data on sediments from 30 lakes in the Altai–Sayan and four neighboring regions showed a significant scatter of the reconstructed Holocene climate parameters. The correlation of changes in the Holocene temperature and in the total solar radiation for plain and mountainous territories was revealed. For mountainous areas, a delayed response of temperature to insolation was noted for the period between 10 and 6.5 ka cal BP, which could be due to the effect of deglaciation. Over the last 12000 years, there was a tendency for climatic humidization because of the combined effect of a decrease in temperature and an increase in precipitation, which could be related to climatic events in the North Atlantic [78].

The reconstruction of the Holocene climate according to palynological studies was performed for the territory of Novosibirsk oblast [66, 77]. For the north, northwest, and northeast of China, schematic maps of climatic humidity were compiled for the periods of 1050–1350 and 1400–1900 AD on the basis of multiple data on 71 studied objects [48]. Application of the CCSM4 model in assessing China's climate change with the use of data for the period from 850 to 1850 AD indicated that precipitation is subjected to unpredictable intradecadal variability, and temperature variability depends on slowly changing interdecadal dynamics of factors [76]. For neighboring Mongolia, a review of extensive data on the Holocene climate obtained from the analysis of different geoarchives was performed. It was concluded that characteristics of the regional paleoclimate change within distances of about 100 km and within several on the time scale, so that the obtained data remain ambiguous for Mongolia and require further studies [59]. The same might be said for the Altai region.

In this paper, the results of pedological and geochemical studies of the soils buried under kurgans of the Srostki-I necropolis (one of the large early medieval necropolises of the Altai region) and reconstruction of the climatic conditions of that period are presented. To identify the localization of cultural monuments of the medieval Srostki community, GIS technologies are used.

The elemental composition of soils is one of the indicators of soil formation and the environmental

conditions, under which the soil formation takes place. Element ratios in the background surface soils and soils buried in different periods are indicative of the conditions of soil formation and sedimentation. Geochemical methods are applied in paleogeographic and paleoenvironmental studies of archaeological sites; they help us to judge soil evolution and solve other issues [3, 4, 18, 19, 36, 37, 49–52, 54, 74]. A number of lithochemical indicators of the paleoclimate and soil-forming conditions have been suggested, including various geochemical coefficients [12, 16, 21, 47, 50, 51, 60–62, 65].

The GIS technologies and remote sensing methods are useful in the study of archaeological heritage sites. The possibilities of their application in archeology in Russia and abroad are analyzed [14, 22, 40, 64]. The distribution of monuments of different archaeological cultures in different periods of the Holocene in the Altai Mountains has been described and corresponding maps have been developed. It has been shown that this region was most actively occupied by humans during periods of humid climate [53]. GIS methods proved to be informative for the study of Paleolithic settlements in the mountainous parts of the Altai region. It was demonstrated that localization of human settlements was controlled by the presence of gently sloping areas, their distance to the nearest river (less than 400 m for 77% of the studied monuments) and to the confluence points of watercourses (less than 2 km, 88%), proximity to sources of stone raw materials, and luminance of the territory [14].

The aim of our research was to study the soils buried under kurgans of the early medieval necropolis Srostki-I and compare them with the modern background analogues in order to assess changes in the physicochemical and geochemical properties and reconstruct climatic conditions during the construction of kurgans in the forest-steppe foothill part of the Altai region in the south of Western Siberia. GIS technologies were applied to determine specific features of localization of settlements and necropolises of the medieval Srostki community.

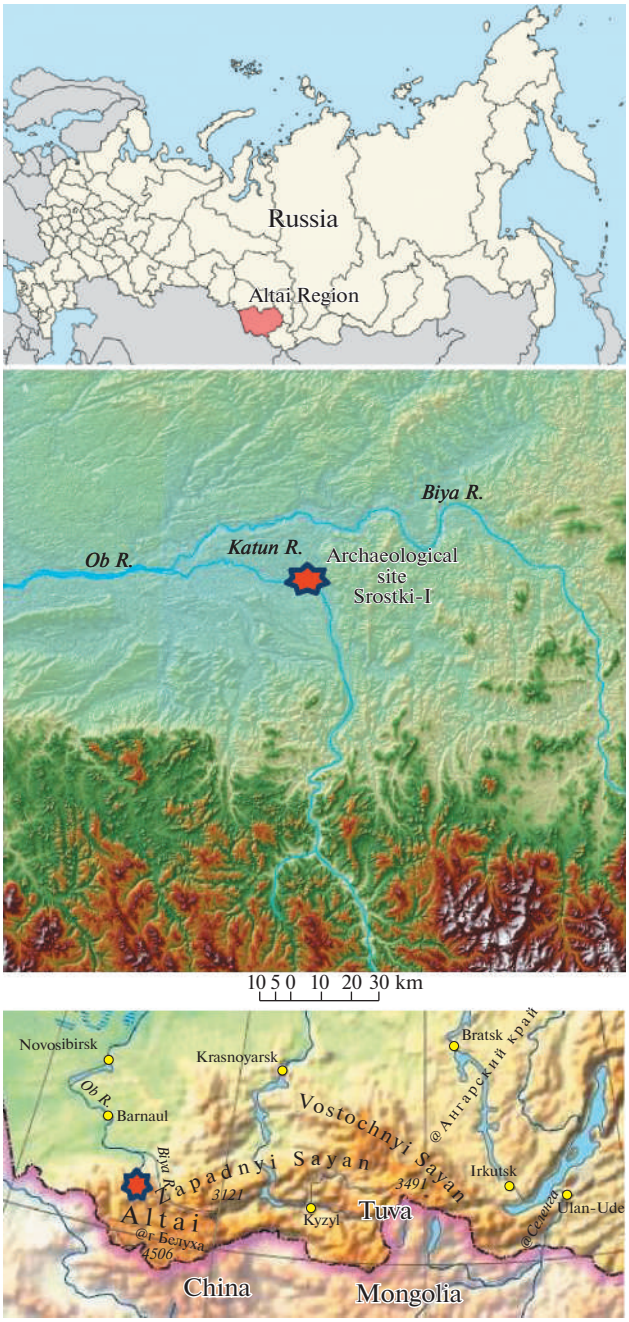


**Fig. 1.** Location of the Srostki-I necropolis.

## OBJECTS AND METHODS

Srostki-I is a group of 61 kurgans dating back to the early medieval period; it is located 25 km southeast from the city of Biysk, on the eastern outskirts of the village of Srostki in Biysk district, on the right bank of the Katun River, on the slope of Mount Piket within the foothill zone of the Biya–Katun interfluve (52°24.337′ N, 85°42.876′ E, 255 m a.s.l.; Fig. 1). Favorable landscape conditions of the transitional zone from the plains to the Altai foothills are largely due to a relatively mild climate with a decrease in annual temperature amplitudes, an increase in precipitation because of the barrier effect, and the transformation of circulation processes. Zonal boundaries have a submeridional direction that repeat the configuration of the mountain ranges.

### *Climate*

According to data from the Biysk weather station, the closest to the Srostki site, the mean January temperature is −13.9°C, the mean July temperature is +20°C, and the mean annual temperature is +3.2°C. The sum of daily active temperatures is 2000–2100°C, and the growing season lasts for 120–130 days. The

mean annual precipitation reaches 548 mm with more than a half in July and August; the difference in annual precipitation between dry and wet years does not exceed 40 mm. Stable snow cover lasts for 165–175 days, its height is 30–60 cm.

The composition of biocenoses on the studied pasture plot with moderate grazing pressure near the necropolis is close to that on virgin land.

### *GIS Methodology*

Multispectral images of Landsat 7 and Landsat 8 satellites with a spatial resolution of 30 m were used. The processing was performed by the synthesis method using ENVI 5.2 software packages. Georeferencing of the source material was completed by finding reference points both on the source georeferenced and processed images. A mosaic of Landsat 7 and Landsat 8 images was compiled and overlain with the following maps: forest vegetation zoning (scale 1 : 2100000), natural zones, soil (scale 1 : 1000000), and mineral resources (scale 1 : 2500000). The geographical location of cultural heritage sites was marked with use of ENVI or ErdasEmagine, Multispec, and QGis software on the obtained electronic cartographic material. A more detailed description of the applied GIS methods was published earlier [40].

### *Soil Study*

Samples of the background soil and two soils buried under kurgans no. 18 and 32 were taken by layers with due account for the boundaries of the genetic horizons: from each 10 cm to a depth of 1 m and from each 20 cm at the depth of 1–2.4 m from three walls of the soil pits.

The studied soils are developed from the loesslike carbonate loams of the Late Neopleistocene–Holocene age forming the covering layer of 2–4 m in thickness. The morphogenetic features of the soils (thickness of individual horizons, distribution of soil humus, color, structure, bulk density, and the presence and morphology of carbonate concentrations) were thoroughly described.

The main soil properties were studied at the Center for Collective Use of the Institute of Physicochemical and Biological Problems in Soil Science, Russian Academy of Sciences. The organic carbon content ($C_{org}$) was determined by Turin's (wet combustion) method; the soil pH, by potentiometry in soil water suspensions (1 : 2.5) and in soil water extracts (1 : 5); the $CO_2$ of carbonates, by titration; the soil particle-size distribution, by the Kachinskii pipette method with pyrophosphate pretreatments; the exchangeable cations, by the Shollenberger method with the subsequent determination of $Ca^{2+}$ and $Mg^{2+}$ by trilonometry and $Na^+$ and $K^+$ by flame photometry; available phosphorus, by Machigin's method (extraction with 1% ammonium carbonate at pH 9 with photometric ending); available potassium was determined in the same extract on a flame photometer.

### *Geochemical Methods*

The contents of 28 elements in soils was determined by X-ray fluorescence analysis on a Spectroscan Makc-GV spectrometer according to the method for measuring the mass fraction of metals and their oxides in powder samples. A weighed portion (2 g) of soil was ground to powder and placed in a special cuvette. Quantitative calibration was carried out using a set of State Standard Soil Samples. The analysis was performed in the Center for Collective Use of the Institute of Physicochemical and Biological Problems in Soil Science by P.I. Kalinin.

The values of the eluvial-accumulative coefficients ($K_{ea}$) were calculated as the ratio of the content of elements in the soil layer, including their average content in the layer of 0–30 cm, to the content of these elements in the parent material. Data on the contents of elements in the studied soils were compared with natural abundances (clarkes) of these elements in the lithosphere; for Si, Al, Fe, Na, Ca, K, Ti, Rb, Zr, and Nb, the latter were taken from Vinogradov [7]; for Mg, Ba, and Cd, from Rudnick and Gao [67]; for Mn, P, Cr, Ni, Zn, As, Sr, and Pb, from Grigor'ev [9]; for V, Co, Cu, and Cs, from Hu and Gao [56]; and for S and Sn, from Wedepohl [74].

The clarkes of concentration of elements—the ratios of their contents in soil horizons to their natural abundances in the lithosphere—were calculated; the reciprocal ratios (the ratios of the natural abundances of elements in the lithosphere to their contents in the soils), or the clarkes of element dispersion were also calculated. The geochemical coefficients based on molar ratios were used.

## RESULTS

### *Radiocarbon Dating and Localization of Monuments of the Srostki Culture*

Radiocarbon dating showed that the objects of historical heritage of the Srostki culture belong to the second half of the 8th–12th centuries. Gryaznov (cited from [38]) was the first to justify the distinction of the Srostki culture and named it based on the results of his excavations.

Using GIS technology, the location of 130 kurgans and necropolises and 21 settlements of the Srostki culture was studied (Fig. S1). The oecumene of the community was mainly in the West Siberian subtaiga–forest-steppe zones. The settlements were located near large lakes and rivers (Ob, Katun, Biya, Alei, etc.) and in places of their junction with smaller watercourses. Such areas are characterized by wide valleys with numerous channels, oxbow lakes, and unflooded parts

**Table 1.** Radiocarbon dating of kurgan samples, AD

| Laboratory index | Sample description | Uncalibrated age | Calibrated age, probability | |
|---|---|---|---|---|
| | | | 1δ, 68% | 2δ, 95% |
| IMKES-14C951 | Remains of wooden pile no. 2, kurgan no. 16 | 860 ± 50 | 890 ± 105 | 885 ± 115 |
| IMKES-14C979 | Human bones, kurgan no. 8, pit no. 2 | 965 ± 90 | 975 ± 85 | 1000 ± 220 |

of terraces with fertile soils for cattle grazing and crop growing. Permanent settlements and large hillforts were constructed. The soil was tilled with a hoe (iron hoes and cultivator points with different bushings were found in the settlement of Elbank). At the Inya-1 site, a vessel filled with grain was found in one of the burial pits, though this is not direct evidence of the development of agriculture [38].

An important occupation of this ethnos was blacksmithing and bronze foundry. This can be proved by a wide range of finds in burials. Several settlements were located within 30–50 km from mineral deposits such as copper, zinc, iron, gold, coal, and clay (Table S1, Figs. S2 and S3). However, most villages were situated at a distance of 90–160 km from the sources of polymetallic ores and precious metals at the foothills and in the mountainous parts of Altai.

A synthesis of data on 24 fortified settlements of the 9th–10th centuries AD in central Europe revealed that they were located both on river floodplains and on tops of the hills. Around the fortified settlements, there was a network of agricultural settlements. Presumably, the population of the settlements was from 50–100 to 3000–4000 inhabitants [55]. In eastern Europe, on the floodplain and on the terraces of the Dnieper River, there was a large medieval settlement Gnezdovo [20].

According to radiocarbon analysis of bone and wood samples from kurgans of the Srostki-I necropolis, it dates back to 890 ± 105 to 975 ± 85 AD (calibration according to 1δ) (Table 1). A recent study of four kurgans allowed to conclude that they were constructed during the Gryaznovo stage, when the consolidation and territorial expansion of the Srostki tribes occurred [8, 38].

### *Soil Studies*

The profile of modern background soil was studied 70 m from the kurgans. The soil had the following horizonation: AO (0–2 cm), A1 (2–20 cm), AB (20–35 cm), B1 (35–50 cm), B2ca (50–80 cm), BCca (80–100 cm), and Cca (100–250 cm). The humus profile of this soil had a small thickness; the soil structure was fine crumb–granular in the A1 and AB horizons, medium crumb in the B1 and B2ca horizons, and coarse crumb in the BCca horizon. The soil effervescence with HCl was observed from the depth of 42–48 cm to the bottom. Carbonate pedofeatures were represented by finely disseminated carbonates, rare soft nodules (white eyes), and calcite crystals (punctuations). In the AB horizon, dark gray tongues extending to 40–50 cm were present.

The kurgan body consisted mainly of the dark gray carbonate-free material of the humus horizon of the ancient soil. The two soils studied under the kurgans slightly differed in their morphology from one another and from the background surface soil. Their humus horizon (A1) had a thickness of about 20 cm, and the soil humus profile (A1 + AB horizons) reached 31–32 cm. The depth of effervescence in the two buried soil was 20–28 and 33–35 cm; both soils contained rare soft carbonate nodules (white eyes), finely disseminated carbonates, and carbonate masses. At the depths of 10–45 cm, wide dark gray humus tongues alternated with reddish brown material.

The investigated background surface and buried paleosols were classified as thin light loamy ordinary chernozems.

**Chemical properties of the background modern soil.** The soil texture is sandy loamy with a predominance of fine and medium sand (0.25–0.01 mm) fractions (75–80%); the contents of fine silt and clay fractions are about 6–10%. These fractions are relatively evenly distributed along the soil profile.

The middle-profile horizons are rich in carbonates with their maximum (7–9% of the $CO_2$ of carbonates) in the layer of 50–120 cm (Fig. 2). Considering the layer-by-layer content of carbonates in the modern and buried soils, close values are observed for soil layers down to a depth of 2.5 m. However, the content of carbonates in the layer of 30–50 cm in the buried paleosols is slightly higher than that in the background surface soils; in the layer of 60–80 cm, it is lower in the buried paleosols.

The soil reaction in the upper horizons is neutral; in the horizons with calcium carbonates, it is alkaline. The cation exchange capacity and the content and composition of the exchangeable cations in the buried paleosols and the background surface soil are similar. The $C_{org}$ content in the surface layer of the background soil is 5.7%; it remains higher than 1% down to the depth of 60 cm. The reconstructed $C_{org}$ content in the upper 50 cm of the buried paleosols is approximately equal to that in the background surface soil (taking into account that about 50% of humus could be mineralized in the past 1000 years) [15]. The $C_{org}$ content in the upper 10 cm of the paleosols is 2.37%; thus, the recalculated initial $C_{org}$ in this layer could reach 5.6%

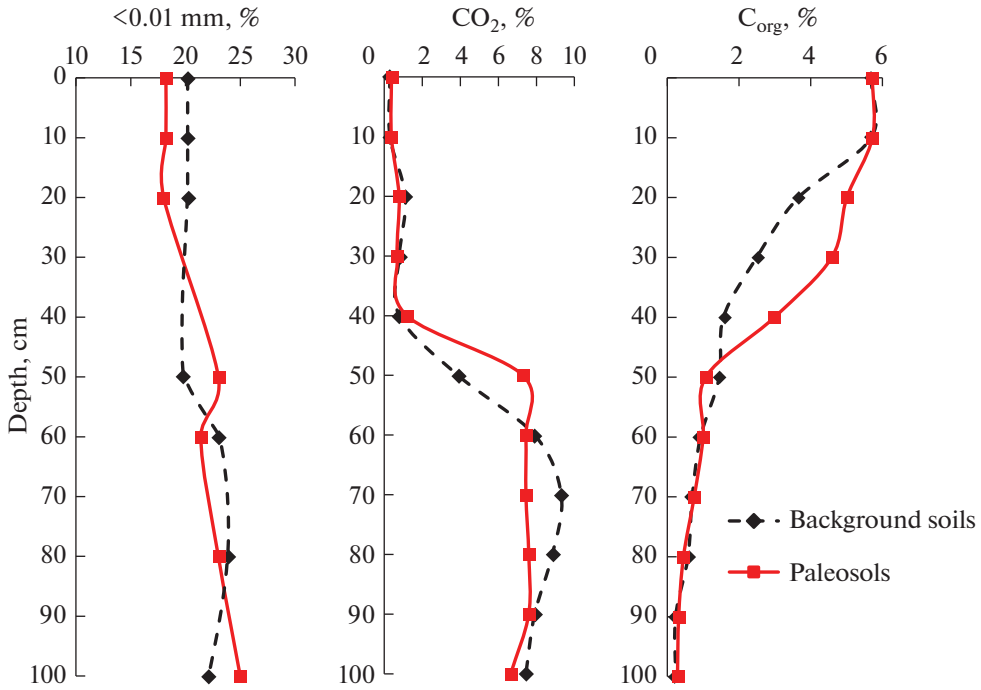


**Fig. 2.** Distribution of the fraction <0.01 mm, $CO_2$ of carbonates, and organic matter ($C_{org}$) in the profiles of studied soils.

**Chemical elements of the soils.** The distribution of different chemical elements in the background soil profile varies (Table 2). Macroelements Si, Al, Fe have a weakly differentiated type of distribution ($K_{ea}$ in the layer of 0–30 cm is 1.1). The distribution of Na is also weakly differentiated ($K_{ea} = 0.9$) with a tendency for Na depletion from the upper layer (0–30 cm) in comparison with the parent material. The contents of Ca and Mg in the upper layer are lower ($K_{ea} = 0.5$–$0.6$), and the content of K is greater ($K_{ea} = 1.3$) than the contents of the corresponding elements in the parent material.

The distribution of trace elements Ni, Pb, Zr, Co in the profile of the background modern chernozem is relatively even (Table 3). The accumulation of S, Rb, Zn, P, K, Mn, Cr, Cu, Ba is observed in all soil horizons in comparison with the parent material. In the humus horizon of the background chernozem, the content of S is higher than its content in the parent material by 4.0–6.1 times; of Rb, by 2.1–2.2 times; of Zn, by 1.5–1.7 times; the contents of P, K, and Cu, by 1.3–1.5 times; of Mn, Cr, Ba, and V, by 1.2–1.3 times; and the content of Ti, by 1.1–1.2 times (Table 4). The

**Table 2.** Macroelemental composition of modern and buried soils, %

| Depth, cm | Si | Al | Fe | Na | $Ca_{cf}/Ca_{tot}$* | Mg | Mn | P | K | S | Ti |
|---|---|---|---|---|---|---|---|---|---|---|---|
| Buried paleosol, pit 9 | | | | | | | | | | | |
| 0–10 | 29.2 | 6.6 | 4.5 | 0.98 | 1.1/1.8 | 1.19 | **0.104** | **0.12** | 1.8 | **0.106** | **0.54** |
| 10–20 | 29.5 | 6.7 | 4.6 | 0.94 | 0.9/1.7 | 1.17 | **0.100** | **0.10** | 1.8 | 0.071 | **0.56** |
| 40–50 | 25.2 | 5.6 | 3.9 | 0.90 | 1.9/8.6 | 1.62 | **0.083** | **0.10** | 1.4 | 0.050 | **0.47** |
| 120–140 | 26.5 | 6.1 | 4.1 | 1.04 | 2.7/7.9 | 1.84 | **0.088** | **0.09** | 1.4 | 0.014 | **0.51** |
| 0–10 | 29.2 | 6.6 | 4.5 | 0.98 | 1.1/1.8 | 1.19 | **0.104** | **0.12** | 1.8 | **0.106** | **0.54** |
| Background surface soil (ordinary chernozem), pit 11 | | | | | | | | | | | |
| 10–20 | 28.9 | 6.4 | 4.5 | 0.88 | 0.7/1.7 | 1.09 | **0.109** | **0.14** | 1.8 | **0.141** | **0.53** |
| 20–30 | 29.4 | 6.8 | 4.6 | 0.85 | 0.8/1.5 | 1.06 | **0.103** | **0.12** | 1.8 | 0.091 | **0.55** |
| 30–40 | 29.5 | 7.0 | 4.7 | 0.96 | 0.7/1.4 | 1.16 | **0.099** | **0.1** | 1.8 | 0.076 | **0.56** |
| 40–50 | 27.4 | 6.2 | 4.3 | 0.89 | 1.5/5.1 | 1.39 | **0.094** | **0.11** | 1.6 | 0.068 | **0.51** |
| Clarke (lithosphere) | 29.5 | 8.05 | 4.65 | 2.50 | 2.96 | 1.49 | 0.077 | 0.07 | 2.5 | 0.095 | 0.45 |

* $Ca_{cf}$—carbonate-free Ca; $Ca_{tot}$—total Ca.
Bold face indicates that the element content in the soil exceeds its clarke in the lithosphere.

**Table 3.** Microelemental composition of modern and buried soils, mg/kg

| Depth, cm | V | Cr | Co | Ni | Cu | Zn | As | Rb | Sr | Ba | Pb | Zr | Sn | Cd | Cs | Nb |
|---|---|---|---|---|---|---|---|---|---|---|---|---|---|---|---|---|
| Buried paleosol, pit 9 | | | | | | | | | | | | | | | | |
| 0–10 | 105 | 69 | 15 | **53** | 16 | **99** | **9.4** | 46 | 194 | **912** | 5.6 | **199** | 1.2 | – | – | – |
| 10–20 | 105 | 67 | **17** | **58** | 16 | **95** | 4.5 | 44 | 200 | **927** | 5.3 | **203** | **11.3** | **0.38** | 3.9 | 9.0 |
| 40–50 | 84 | 52 | **19** | **57** | 14 | 61 | **6.5** | 28 | 266 | **759** | 5.3 | **191** | **7.4** | **0.27** | 4.7 | 6.0 |
| 120–140 | 91 | 80 | **19** | **57** | 14 | 69 | **7.0** | 22 | 326 | **783** | 5.5 | **189** | – | **0.48** | 4.0 | 8.3 |
| Background surface soil (ordinary chernozem), pit 11 | | | | | | | | | | | | | | | | |
| 10–20 | 101 | 70 | **19** | **55** | 15 | **95** | 4.0 | 47 | 198 | **941** | 5.5 | **202** | **11.0** | **0.44** | 4.0 | 13.7 |
| 20–30 | 104 | 71 | **19** | **58** | 15 | **104** | – | 45 | 193 | **935** | 5.4 | **202** | **11.1** | **0.40** | 3.6 | 8.5 |
| 30–40 | 107 | 75 | **18** | **61** | 14 | **96** | – | 45 | 190 | **944** | 5.2 | **204** | **12.0** | **0.38** | 3.9 | 13.8 |
| 40–50 | 96 | 69 | **16** | **56** | 13 | **82** | 5.6 | 39 | 207 | **853** | 5.3 | **206** | **8.0** | **0.38** | 4.3 | 9.5 |
| 90–100 | 88 | 57 | **19** | **59** | 11 | 62 | **7.1** | 21 | 310 | **757** | 5.5 | **193** | – | **0.49** | 4.5 | 6.3 |
| Clarke (lithosphere) | 106 | 92 | 15 | 50 | 27 | 75 | 5.6 | 150 | 270 | 628 | 17 | 170 | 2.5 | 0.09 | 4.9 | 20 |
| Clarke (regional soils)[a] | 129 | 60 | 11 | 29 | 39 | 70 | 6.8 | 68 | 175 | 460 | 27 | 267 | 2.5 | 0.41 | 5.1 | 12 |
| Clarke (chernozems of the USSR)[b] | 37–125 | 71–195 | 0.5–50 av. 12 | 14–40 | 16–70 | 39–82 | – | – | 520–3500 | 475–620 | 10–67* | 224^ | 0.2–5 av. 1.4 | 0.01–0.07 | 0.3–5.1/ 2.2–16.7# | – |

Natural abundances (clarke values) for regional soils [(a)] are given according to [16, 33]; for chernozems of the Soviet Union [(b)] and world soils [(c)], according to [ ]; for Zr [(^)], the data are from the United States; for Cs [(#)], from Canada/Bulgaria; for Pb [(*)], from different soils according to [57]. Bold face indicates the values that are higher than natural element abundances in the lithosphere.

**Table 4.** Element contents in different soil layers in comparison with the parent material (eluvial–accumulative coefficients)

| Depth, cm | Si | Al | Fe | Na | Ca | Mg | Mn | P | K | S | Ti | V | Cr | Co | Ni | Cu | Zn | As | Rb | Sr | Ba | Pb | Zr | Cd | Cs | Nb |
|---|---|---|---|---|---|---|---|---|---|---|---|---|---|---|---|---|---|---|---|---|---|---|---|---|---|---|
| Buried paleosol, pit 9 | | | | | | | | | | | | | | | | | | | | | | | | | | |
| 0–10 | 1.1 | 1.1 | 1.1 | 0.9 | 0.4 | 0.65 | 1.2 | 1.3 | 1.2 | 7.6 | 1.1 | 1.2 | 0.9 | 0.8 | 0.9 | 1.1 | 1.4 | 1.3 | 2.1 | 0.6 | 1.2 | 1.0 | 1.1 | – | – | – |
| 10–20 | 1.1 | 1.1 | 1.1 | 0.9 | 0.4 | 0.6 | 1.1 | 1.1 | 1.2 | 5.1 | 1.1 | 1.2 | 0.8 | 0.9 | 1.0 | 1.1 | 1.4 | 0.6 | 2.0 | 0.6 | 1.2 | 1.0 | 1.1 | 0.8 | 1.0 | 1.1 |
| 40–50 | 1.0 | 0.9 | 1.0 | 0.9 | 0.7 | 0.9 | 0.9 | 1.1 | 1.0 | 3.6 | 0.9 | 0.9 | 0.7 | 1.0 | 1.0 | 1.0 | 0.9 | 0.9 | 1.3 | 0.8 | 1.0 | 1.0 | 1.0 | 0.6 | 1.2 | 0.7 |
| Background surface soil (ordinary chernozem), pit 11 | | | | | | | | | | | | | | | | | | | | | | | | | | |
| 10–20 | 1.1 | 1.1 | 1.1 | 0.02 | 0.5 | 0.6 | 1.3 | 1.5 | 1.3 | 6.1 | 1.1 | 1.2 | 1.2 | 1.0 | 0.9 | 1.4 | 1.5 | 0.6 | 2.2 | 0.6 | 1.2 | 1.0 | 1.0 | 0.9 | 0.9 | 2.2 |
| 20–30 | 1.1 | 1.2 | 1.1 | 0.9 | 0.5 | 0.6 | 1.2 | 1.3 | 1.3 | 4.0 | 1.1 | 1.2 | 1.2 | 1.0 | 1.0 | 1.4 | 1.7 | – | 2.1 | 0.6 | 1.2 | 1.0 | 1.0 | 0.8 | 0.8 | 1.4 |
| 30–40 | 1.1 | 1.2 | 1.2 | 1.0 | 0.5 | 0.7 | 1.2 | 1.2 | 1.3 | 3.3 | 1.1 | 1.2 | 1.3 | 1.0 | 1.0 | 1.3 | 1.5 | – | 2.2 | 0.6 | 1.2 | 1.0 | 1.1 | 0.8 | 0.9 | 2.2 |
| 40–50 | 1.1 | 1.1 | 1.1 | 0.9 | 1.0 | 0.8 | 1.1 | 1.2 | 1.2 | 3.0 | 1.0 | 1.1 | 1.2 | 0.8 | 1.0 | 1.2 | 1.3 | 0.8 | 1.9 | 0.7 | 1.1 | 1.0 | 1.1 | 0.8 | 1.0 | 1.5 |

eluvial type of distribution in the upper horizons of the background soil is typical for alkaline and alkaline-earth elements: $K_{ea}$ is 0.8–0.9 for Na, Cs, and Cd;0.6 for Mg and Sr; and 0.5 for Ca. Arsenic is also depleted from the soil profile in comparison with the parent material ($K_{ea}$ = 0.2–0.6). for As.

In the soil buried under the kurgans, the elemental composition differs from that in the background surface soil. In the upper horizons of the medieval soil, the contents of P, S, Cr, and Co are slightly lower than in the background chernozem; in the lower horizons, the contents of Ca and Mg are somewhat higher than in the background chernozem at corresponding depths. In contrast to the background analogue, the removal of Co and Cr from the soil in comparison with the parent material is observed in the buried soil. A small accumulation of As is seen in the upper (0–10 cm) layer of the buried soil in comparison with the background chernozem. Distribution patterns of other elements in the buried soils do not differ from those in the background surface soils.

**Comparison with natural element abundances in the lithosphere.** In the background chernozem, the contents of Mn, P, Ti, Cd, Ba, Zr, Co, and Ni are higher than their clarke values in the earth's crust. At the same time, the excess of S above the clarke is observed only in the uppermost 10-cm-thick layer. On the contrary, the contents of As, Mg, and Sr are higher than their clarke values only in the parent material. The content of Zn in the humus and middle-profile horizons exceeds its clarke; at the depth of 90–100 cm, it becomes less than the clarke of this element in the lithosphere. According to the relative abundances (clarkes of concentration) of the elements in the upper 20-cm-thick layer of the background chernozem, the elements are arranged in the following order: Cd 4.9 > P 2.0 > Ba, S 1.5 > Mn, Zn 1.3–1.4 > Co 1.3 > Zr 1.2 > Ni 1.1.

The contents of Si and V in the background chernozem are approximately equal to their natural abundances in the lithosphere. The contents of Al, Fe, Na, K, Cr, Cu, Sr, Pb, Cs, Nb, and Rb are lower than their natural abundances in the lithosphere. This indicates the dispersion of these elements within the profile of modern chernozem in comparison with the lithosphere. According to the value of the clarke of dispersion, the elements in the upper 20-cm-thick layer of the background chernozem are distributed in the following order: Ca 4.2 > Rb and Pb 3.1–3.2 > Na 2.8 > Nb 1.5 > Cu 1.8 > Mg, K, As, Sr 1.4 > Cr, Cs, Al, Fe 1.2–1.3.

The clarkes of concentration and dispersion of the elements in the soil buried under the kurgan are almost the same as those in the background surface soil.

## DISCUSSION

### *Soil Characteristics*

The current soil cover of the site is relatively uniform. This is due to the properties of loess soil-forming material, as well as to a relatively smooth topography of the interfluve, to which the necropolis is confined. A comparison of the morphological properties of buried and background soils indicates that they differ slightly in the depth of carbonates.

The diagenetic processes in soils that were buried under the kurgans caused a gradual decrease in the humus content due to its mineralization and the lack of input of fresh plant residues. It was previously shown that the humus horizon soils buried 1000 years ago contains about 50% of the initial amount of $C_{org}$ [15]. The mineralization rate is also affected by the composition of humus in the paleosols: free and loosely bound $C_{org}$ is mineralized faster, while $C_{org}$ bound with clay minerals forms a passive carbon pool and is preserved much longer.

The reconstructed $C_{org}$ content in the upper 50-cm-thick layer of paleosols is approximately equal to its amount in the background soil considering that about 50% of humus was mineralized over 1000 years. In the paleosols, there is a slight accumulation of carbonates at a depth of 30–50 cm and some depletion of carbonates from the layer of 60–80 cm. Therefore, the average $CaCO_3$ content in the 1-m-thick (4.9%) of the

background and ancient soils does not differ. The accumulation of organic matter in these soils is alike. Some increase in the content of carbonates in the layer of 30–50 cm of the paleosols indicates that soil formation in the period before the construction of kurgans proceeded under somewhat drier conditions. However, this period was short, because the soil humus had no enough time for mineralization to get in equilibrium with the onset of drier conditions.

### *Elemental Composition of Soils*

The elemental composition of the paleosol is very similar to its modern analogue. The contents of P, S, Co, and Cr in the upper horizons of the soil buried under the kurgan are slightly lower than those in the corresponding horizons of the background chernozem. Phosphorus and sulfur are biophilous elements; they are intensively absorbed by plant roots. The concentrations of P and S in plant ash are $10^1$–$10^2$ times higher than those in the soil (according to Perelman (1961)); after dying of the plants, these elements accumulate in the humus horizon. In particular, wormwood of steppe landscapes actively accumulates these elements [18]. Apparently, the accumulation of biogenic elements in the soils buried under the kurgans was less pronounced than that in the background surface soil. However, the concentration of S in the upper soil horizons in comparison with the parent material ($K_{ea}$) in the medieval soils was higher than that in the background modern soil. In general, a less intensive accumulation of biophilous elements in the surface layer of the paleosol in comparison with the background surface soil may be indicative of a drier climate in the period before the construction of the kurgans. At the same time, a higher eluvial-accumulative coefficient for S in the paleosol attests to some humidization of the climatic conditions.

The intensity of accumulation of Mg, K, and Ca in the surface horizons of the buried paleosols and the background surface soil in comparison with the parent material is similar. The concentration of these elements tends to be high in plants. However, these elements can be washed off from the soil profile with an increase in humidity of the climate. A weaker degree of leaching of carbonates from the middle-profile horizons of the buried paleosols in comparison with the background surface soil attests to a somewhat higher aridity of the climate during the early medieval period.

Among hazardous pollutants of the first class of toxicity (As, Pb, Cd), the studied soils are enriched with Cd in comparison with its clarke in the lithosphere, though Cd concentration in them is close to the average concentration of Cd in soils of the world. The contents of Cd and As in the soil horizons are lower than those in the parent material; the content of Pb in the soil horizons is the same as in the parent material. The concentration of Cd in the background surface soil and in the buried paleosol is considerably lower than the tentative permissible concentration (10 mg/kg), and the concentration of As in the topsoil (0–10 cm) reaches 9.4 mg/kg and approaches the tentative permissible concentration (10 mg/kg) [58]. It should be noted that, in general, the soils of the studied region are relatively rich in As. The average content of As in soils of the south of Western Siberia reaches 13 mg/kg [37]. At the same time, the share of easily soluble As compounds in these soils is <1% increasing up to 10% in the technogenically contaminated soils [16].

The contents of Zn, Ba, Sn, and Ni in the studied soils are higher, and the contents of Cu, Zr, and Pb are lower than the average contents of these elements in soils of the region. The accumulation of Zn, Ba, Sn, and Ni in the studied soils is observed despite the low content of clay particles. It is known that most of the considered trace elements are accumulated in the clay fraction of the soils, being part of clay minerals or being adsorbed on the surface of clay particles.

In the studied background and buried chernozems, the concentrations of Fe, Na, Ca, Mg, Mn, P, K, S, Sn, Ti, Co, Ni, Zn, and Ba are higher in comparison with average concentrations of these elements in soils of the world. On the contrary, the concentrations of Al, Cr, Cu, Sr, Pb, Cs, Rb, Zr, and Nb are lower, and the concentrations of Si, V, and Cd are close to the average concentrations of corresponding elements in soils of the world.

The main factors that determine the concentration of elements in soils are the chemical and mineralogical compositions of parent rocks and the dispersion degree of the substrate. It was shown that the distribution of elements in the soil profiles and their accumulation in the topsoil (0–20 cm) in the south of Western Siberia are determined by contents of physical clay (<0.01 mm) and clay (<0.001 mm) particles, cation exchange capacity, and, to a lesser extent, by the humus content. A strong correlation of the distribution of Cu and Zn in the soil profiles with the distribution of Fe was found [1]. At the same time, positive correlation of the contents of Co, Mn, Zr, Mo and, to a lesser extent, Zn and Pb with the contents of sand and coarse silt fractions was found for heavy loamy chernozem soils of Tula oblast. No such correlation was noted for Ni, Cr, Ti, and Fe [35].

Thus, the enrichment with Zn, Ba, Sn, and Ni of the studied soils with respect to the regional average value should be linked to the local natural features of the parent material dictating the elemental composition of the soils. The depletion of Cu and Pb in the soils buried under the kurgans and in the background modern chernozems in comparison with the average regional values is related to a relatively coarse texture of the studied soils.

It should be noted that no enrichment of the background soil with highly hazardous chemical elements in comparison with the buried analogues of the medi-

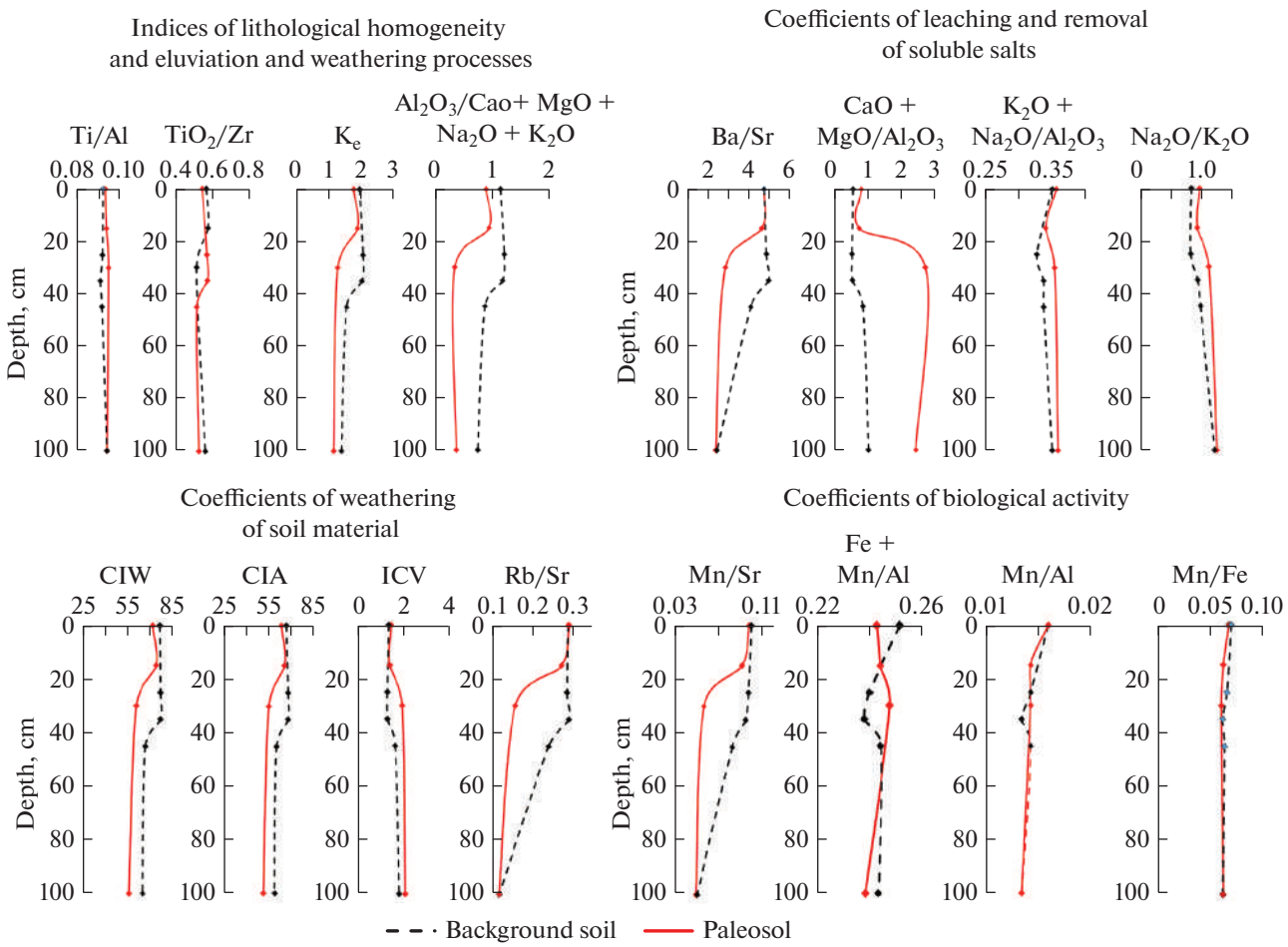


**Fig. 3.** Distribution of the values of some geochemical coefficients in the profiles of background surface soil and paleosol buried under the kurgan.

eval necropolis of Srostki-I has been observed. At the same time, there are data on the accumulation of some heavy metals in buried paleosols in different parts of the world. Thus, a study of chestnut soils buried under kurgans in the Volga region demonstrated that these soils are enriched in mobile forms of Pb, though the total Pb content in them is not increased. A shift in the isotopic composition of mobile Pb towards less radiogenic values took place upon the transition from the Bronze Age to the Early Iron Age and to the modern background soils, which could be due to the enhanced atmospheric transport and deposition of Pb compounds [28]. Studies conducted in Sweden showed that Pb pollution of lake sediments began 2 000 years ago with the industrial development; since 900 AD, there has been a continuous increase in atmospheric deposition of anthropogenic Pb compounds in Europe [44].

### *Geochemical Coefficients*

Geochemical indicators were calculated in order to reconstruct the climatic conditions of soil formation in the Medieval Ages (Table 5). The values of Ti/Zr and Ti/Al ratios in different horizons of the studied soils are approximately the same, which indicates the lithological homogeneity of the soil stratum. This allows us to evaluate the changes in soil formation conditions, including climate, by other geochemical indicators.

The averaged value of the $Al_2O_3/(CaO + MgO + Na_2O + K_2O)$ ratio in the upper 30 cm is slightly lower in the soil buried under the kurgan than in the background surface soil. This attests to a weaker degree of mineral weathering in the soil of the Medieval Ages. The chemical index of alteration $CIA = Al_2O_3 \cdot 100/(Al_2O_3 + CaO + Na_2O + K_2O)$ has maximum values in the upper horizons of the background chernozem and decreases down the soil profile (Fig. 3). In the buried paleosol, the CIA values are slightly lower than those in the background surface soil. A comparison of the averaged values of geochemical coefficients in the layer of 0–30 cm relative to their values in the parent materials is more informative. Though the difference between the modern soil and the buried paleosol

**Table 5.** Geochemical coefficients, their formulas and references, their weighted mean values in the layer of 0–30 cm (above the line), and the ratios of their values in this layer to their values in the parent material (under the line) for the background surface chernozems and for paleochernozems buried under the medieval kurgans

| Coefficient | | Background | Paleosol | Author |
|---|---|---|---|---|
| $CIA = Al_2O_3 \times 100/(Al_2O_3 + CaO + Na_2O + K_2O)$ | Weathering coefficients: ratios of minerals more resistant to weathering (represented by Al) to less stable minerals (associated with Ca, Mg, Na, and K) | 67/1.14 | 64/1.25 | Nesbitt and Young, 1982 [61] |
| $CIW = 100 \times Al_2O_3/(Al_2O_3 + CaO + Na_2O)$ | | 77/1.18 | 73/1.30 | Visser and Young, 1990 [72] |
| $PWI = (4.20Na + 1.66Mg + 5.54K + 2.05Ca) \times 100$ | | 58/0.6 | 60/0.7 | Gallagher and Sheldon, 2013 [50, 51] |
| $W = [(0.203 \times \ln(SiO_2) + 0.191 \times \ln(TiO_2) + 0.296 \times \ln(Al_2O_3) + 0.215 \times \ln(Fe_2O_3) - 0.002 \times \ln(MgO) - 0.448 \times \ln(CaO) - 0.464 \times \ln(Na_2O) + 0.008 \times \ln(K_2O) - 1.374]$ | | 0.52/17.3<br>0.08/–0.20 | 0.38/0.41<br>–0.11/0.16 | Tohru and Hiroyoshi, 2007 [71] |
| $ICV = (Fe_2O_3 + CaO + MgO + Na_2O + K_2O + TiO_2)/Al_2O_3$ | | 1.28/0.72 | 1.38/0.67 | Cox et al., 1995 [49] |
| $Al_2O_3/(CaO + MgO + Na_2O + K_2O)$ | | 1.17/1.58 | 1.05/1.71 | Retallack, 2003 [64] |
| $SiO_2/Al_2O_3$ | | 8.5/1.00 | 8.5/1.01 | |
| Rb/Sr | | 0.24/3.45 | 0.23/3.42 | Gallet, 1996 [51] |
| Ba/Sr | Indicators of hydrothermal conditions and leaching processes | 4.8/1.97 | 4.7/1.96 | Retallack, 2003 [64] |
| Sr/Ba | | 0.20/0.50 | 0.20/0.50 | Dobrovolskii, 1984 [12] |
| MnO/Sr | Coefficients of biological activity | 0.10/1.97 | 0.09/1.92 | Retallack, 2003 [64] |
| (Fe + Mn)/Fe | | 1.07/1.00 | 1.07/1.00 | |
| Mn/Fe | | 0.07/1.09 | 0.07/1.04 | |
| Mn/Al | | 0.016/1.14 | 0.015/1.07 | |
| Na/K | Indices of the removal of soluble salts | 0.81/0.69 | 0.92/0.76 | |
| Na/Al | | 0.15/0.80 | 0.17/0.85 | |
| (K + Na)/Al | | 0.34/0.97 | 0.35/0.97 | |
| (Ca + Mg)/Al | Index of transformation of carbonates | 0.52/0.52 | 0.61/0.48 | |
| Ti/Al | Indices of lithological homogeneity of the material | 0.09/0.98 | 0.09/0.99 | Schilman et al, 2001 [67] |
| Ti/Zr | | 0.56/0.97 | 0.57/1.02 | Hutton (cited from [57]) |
| $CaO/Al_2O_3$ | Geochemical indices of pedogenesis | 0.15/0.43 | 0.21/0.34 | Eze and Meadows, 2014 [49] |
| $Ke = Al_2O_3/(MnO + CaO + K_2O + MgO + Na_2O)$ | Eluviation coefficient | 2.0/1.44 | 1.8/1.59 | Liu et. al., 2009 [60] |
| $Km = \sum(Na, K, Mg, Zn)/SiO_2$ | Mobility coefficient | 1.66/1.39 | 1.61/1.25 | Lisetskii, 2016, 2017 [21, 22] |
| $Fi = (CaO + MgO + 10P_2O_5)/SiO_2$ | Index of potential soil fertility | 0.08/0.62 | 0.09/0.53 | Taylor et. al., 2008 [70] |
| HM = Co + Cr + Cu + Pb + Sr | Sum of heavy metals | 305/0.76 | 302/0.68 | Lisetskii, 2016 [21] |

For index W, the values calculated from data on the contents of element oxides are given above the line, and the values calculated from data on the molar ratios of the oxides are given under the line.

with respect to this indicator is not great, it can be concluded that the paleosol is more differentiated according to the CIA values.

The CIA value reflects the depth of weathering of the mineral part of the soil. In unweathered rocks, the CIA value is about 50, and in highly weathered rocks, it is 100 [62]. High values of CIA suggest a predominant removal of mobile elements ($Ca^{2+}$, $Na^{+}$, and $K^{+}$) during chemical weathering in comparison with more stable elements ($Al^{3+}$ and $Ti^{4+}$) in humid climate. Low CIA values imply an almost complete absence of chemical weathering and, therefore, they can be used as indicators of a cold and/or arid climate. A study of modern and ancient sediments (281 samples) indicated that the CIA value depends on the degree of climatic humidity. However, if the soils or sediments are rich in carbonates (>30%) and contain potassium (owing to diagenetic illitization), the use of CIA as an indicator of paleohumidity of the climate may lead to erroneous conclusions [54].

In the soil profile of the Neolithic–Eneolithic settlement Kochegarovo-1 (7200–5350 years ago, $^{14}C$ cal, 1σ) in the forest-steppe zone of Western Siberia (Kurgan oblast), the CIA values were 65–75; in the background surface soils they reached 75–80 [4]. The values of other geochemical coefficients, such as Ba/Sr, Rb/Sr, and Mn/Sr ratios in the buried paleosol and the modern surface soil do not differ. The Ba/Sr index is based on the fact that the intensity of Ba (element of potassium feldspars) removal is lower than the intensity of Sr (constituent of carbonates) removal [65]. The Rb/Sr index reflects the difference in the resistance of different minerals to weathering; Rb is associated with mica and potassium feldspars, whereas Sr is mainly associated with carbonates [52]. The inverse Sr/Ba ratio is an indicator of changes in the hydrothermic conditions and increases with increasing aridity of the climate [12]. For very arid conditions, this ratio may exceed 10; in the steppe regions it is about 1; in the forest-steppe it is less than 1 [7]. In the profile of the studied paleosol and modern chernozem, the Sr/Ba value is 0.2 in all horizons.

In the layer of 40–50 cm of the buried paleosol, the value of the $(CaO + MgO)/Al_2O_3$ index is increased, which reflects the accumulation of calcite. The $Na_2O/K_2O$ and $Na_2O/Al_2O_3$ ratios are slightly higher in the paleosol than in the modern surface soil, which is indicative of a lower leaching of carbonates and sodium and potassium compounds from the profile of the buried paleosol. However, these ratios are generally low and attest to the absence of soluble salts in the soil profiles. The value of the eluviation coefficient also attests to a lower activity of the leaching of bases from the paleosol profile.

The values of the Mn/Al, Mn/Fe, and $(Fe_2O_3 + MnO)/Fe_2O_3$ ratios are considered to be indicators of the intensity of biological processes with participation of Mn and Fe in the biogenic accumulation and migration. These ratios in the buried paleosol do not differ from those in the background chernozem.

The index of potential soil fertility—$Fi = (CaO + MgO + 10P_2O_5)/SiO_2$ [71] was also calculated. Its values in the buried paleosol and background surface soil are relatively close. At the same time, the ratio of the averaged values of this index in the upper 30 cm and in the parent material is higher in the background chernozem, which may be indicative of the weakened activity of biogenic accumulative processes in the paleosol. The indices of the total content of heavy metals (Co + Cr + Cu + Pb + Sr) [21] in the layers of 0–10 and 0–30 cm in the studied soils are similar. The Sr content is the highest among the considered heavy metals. This element is associated with carbonates; it is possible that its residual accumulation is the upper horizon took place after the removal of calcium carbonates in the course of pedogenesis.

Thus, paleosols are characterized by a lower leaching of carbonates from the middle part of the profile; lower accumulation of biophilous elements, such as P, S, and Co, in the surface layers; and lower values of the weathering indices CIA ($100\ Al_2O_3/(CaO + MgO + Na_2O + K_2O)$) and CIW ($100\ Al_2O_3/(Al_2O_3 + CaO + Na_2O)$) in comparison with the background soil. These characteristics indicate that soil formation before the construction of the medieval kurgans proceeded under somewhat drier climatic conditions in comparison with the modern period. However, general similarity of the buried paleosol and background surface soil in their morphology, reconstructed humus content, and averaged values of the coefficients of weathering and biological activity in the topsoil (0–30 cm) relative their values in the parent material point to the beginning of some humidization of the climate at the time of construction of the kurgans.

The reconstruction of climatic conditions on the basis of pollen spectra from the paleosols buried under kurgans of the Srostki-I necropolis is in agreement with this conclusion. The buried paleosols contain less pollen of pine, birch, and willow in comparison with the modern soils. This may be related to deforestation of the territory in the Medieval Epoch due to cutting of forests, lowed amount of snow and lower water supply of the soils in the spring season, and smaller areas occupied by pine stands because of colder and more severe winters. At the same time, water availability in the summer season was no less than at present, because mesophytic herbs predominated over xerophytic steppe plants. Sedges predominated in mires appearing after drying of shallow lakes, while the water conservation role of forests was decreased. At the same time, there was a slight increase in the amount of pollen of xerophytes, including *Artemisia* and Chenopodioideae species and wild grasses, whose expansion could be due to surface disturbance during the construction of 61 kurgans [24, 32].

The tree-ring chronology "Mongun" for the past 2367 years was developed on the basis of data on the rings of Siberian larch sampled near the upper boundary of this species growing in the Altai–Sayan Mountains. It was shown that the growth of larch correlates well with the early summer temperatures. Temperature conditions were favorable for larch growth during the period of medieval warming in the 7th–10th centuries AD. Severe cooling in June–July took place in 1190–1191; temperature extremes in 969–991 were 1.5°C higher than the average values [25].

The results of these studies allow us to conclude that the development of the Srostki culture in the 8th–12th centuries AD and the period of construction of kurgans of the Srostki-I necropolis were characterized by relatively favorable environmental conditions for this ethnic group, as evidenced by the pedological, geochemical, palynological, and dendrochronological data.

## CONCLUSIONS

A geochemical and physicochemical study of the soils buried under kurgans of the early medieval necropolis Srostki-I and the background surface soils and reconstruction of paleoclimatic conditions of that period were performed.

The paleosols are characterized by a lower leaching of carbonates from the middle-profile horizons; lower accumulation of biophilous elements, such as P, S, and Co, in the surface layers; and lower values of the chemical index of alteration ($Al_2O_3/(CaO + MgO + Na_2O + K_2O)$) in comparison with the background soil. These characteristics indicate that the development of the paleosols in the period before the construction of the kurgans proceeded under somewhat drier climate conditions in comparison with those at present. At the same time, close morphological features of the buried paleosols and background surface soils and data on the reconstructed humus content and averaged values of geochemical indices CIA ($100\ Al_2O_3/(Al_2O_3 + CaO + Na_2O + K_2O)$) and Rb/Sr, as well as geochemical indicators of the intensity of biological processes (Mn/Sr, Mn/Al, and Mn/Fe) in the upper 30 cm relative to their values in the parent material suggest that the period of the increased dryness of the climate was short and that some humidization of the climate began in that period.

The studied soils are characterized by the high contents of Ni, Zn, Ba, and Sn and the low contents of Cu and Pb in comparison with the average contents of these elements in soils of the region, world soils, and the lithosphere. The background surface chernozems and buried paleosols are enriched in As and Cd in comparison with natural abundances of these elements of the first hazard class in the lithosphere, which is generally typical of the regional soils. At the same time, their contents in the studied soils remain below the critical levels endangering human health. The microelemental composition of the soils is largely determined by the chemical, mineralogical, and textural properties of the parent material. No accumulation of toxic elements related to the anthropogenic activity has been noted for the modern background soils in comparison with their medieval analogues.

With the use of GIS technology, the localization of 21 settlements and 130 necropolises of the Srostki community that existed in the studied area during the Viking Age (second half of the 8th–12th centuries AD) was shown on different thematic maps. This study demonstrated that the medieval settlements were located on fertile soils within plain areas with a small amplitude of heights near large lakes and rivers (Ob, Katun, Biya, Alei, etc.) and in widenings of river valleys at the confluence of small streams with larger water bodies.

## ACKNOWLEDGMENTS

The authors are grateful to the participants of the archaeological expedition for their assistance in conducting field work.

## FUNDING

The work was performed within the framework of state contract no, 0191-2019-0046; laboratory analyses and GIS studies were supported by the Russian Foundation for Basic Research (project no. 17-05-01151 and 20-05-00284), and field work and data interpretation were supported by the Russian Science Foundation (project no. 16-18-10033 "Formation and Evolution of Life-Support Systems of Nomadic Societies in the Altai Region and Adjacent Territories during the Late Antique Time and in the Middle Ages: Multiple Reconstruction.".

## CONFLICT OF INTEREST

The authors declare that they have no conflict of interest.

## SUPPLEMENTARY MATERIALS

**Table S1.** The remoteness of settlements of the Srostki community from mineral deposits, km.

**Fig. S1.** Distribution of monuments of the medieval Srostki culture on the soil map of the Altai region (1 : 1 M scale). The soil map was compiled by N.I. Bazilevich, I.I. Karmanov, V.I. Kravtsova, N.V. Orlovskii, and A.N. Rozov. Hereinafter: triangles indicate necropolises, and squares indicate settlements; Site no. 60 is the Srostki-1 necropolis.

**Fig. S2.** Distribution of monuments of the medieval Srostki culture on the map of mineral deposits of the Altai region (1 : 2.5 M scale) compiled by the VSEGINGEO (State Balance of Mineral Resources in the Altai Region for January 10, 2010).

**Fig. S3.** Composition of 21 multispectral Landsat 8 images obtained in 2017 showing the territory of the Altai region.

## REFERENCES


1. Yu. A. Azarenko, *The Content, Distribution, and Relationship of Trace Elements in the Soil-Plant System in the South of Western Siberia* (Variant-Omsk, Omsk, 2013) [in Russian].
2. A. L. Aleksandrovskii, M. A. Bronnikova, Yu. N. Vodyanitskii, M. I. Gerasimova, et al., *Soil as a Memory of the Biosphere–Geosphere–Anthroposphere Interactions*, Ed. by V. O. Targulian and S. V. Goryachkin (LKI, Moscow, 2008) [in Russian].
3. A. O. Alekseev, P. I. Kalinin, and T. V. Alekseeva, "Soil indicators of paleoenvironmental conditions in the south of the East European Plain in the Quaternary time," Eurasian Soil Sci. **52**, 349–358 (2019). https://doi.org/10.1134/S1064229319040021
4. L. R. Bikmulina, A. S. Yakimov, V. S. Mosin, and A. I. Bazhenov, "Geochemical features of soils and cultural layers of the Neolith–Eneolithic settlement Kochegarovo-1 in the forest-park zone of Western Siberia and their paleoecological description," Archaeol. Ethnol. Antropol. Eurasia, No. **2** (45), 35–44 (2017). https://doi.org/10.17746/1563-0110.2017.45.2.035-044
5. M. A. Bronnikova, A. R. Agatova, M. P. Lebedeva, R. K. Nepop, Yu. V. Konoplianikova, and I. V. Turova, "Record of Holocene changes in high-mountain landscapes of southeastern Altai in the soil–sediment sequence of the Boguty River valley," Eurasian Soil Sci. **51**, 1381–1396 (2018). https://doi.org/10.1134/S1064229318120037
6. M. A. Bronnikova, Yu. V. Konoplianikova, A. R. Agatova, E. P. Zazovskaya, M. P. Lebedeva, I. V. Turova, R. K. Nepop, I. G. Shorkunov, and A. E. Cherkinsky, "Coatings in cryoaridic soils and other records of landscape and climate changes in the Ak-Khol Lake basin (Tyva)," Eurasian Soil Sci. **50**, 142–157 (2017). https://doi.org/10.1134/S1064229317020016
7. A. P. Vinogradov, "Average content of chemical elements in general types of erupted minerals of the Earth crust," Geokhimiya, No. 7, 555–571 (1962).
8. V. V. Gorbunov, A. A. Tishkin, and A.L. Kungurov, "Settlements of the Srostki culture in forest-steppe Altai: identification signs," Izv. Altai. Gos. Univ., No. 4 (92), 218–229 (2016). https://doi.org/10.14258/izvasu(2016)4-38
9. N. A. Grigor'ev, *Distribution of Chemical Elements in the Upper Part of Continental Crust* (Ural Branch, Russian Academy of Sciences, Yekaterinburg, 2009) [in Russian].
10. M. I. Dergacheva and K. O. Ochur, "Reconstruction of the environmental dynamics in the central Tuva Depression in the Holocene," Vestn. Tomsk. Gos. Univ., Biol., No. 1, 5–17 (2012).
11. M. I. Degacheva, I. N. Fedeneva, and N. V. Goncharova, "Evolution of the environment in the northwestern and central Altai in the Late Pleistocene and Holocene," Geogr. Prirod. Resur., No. 1, 76–83 (2003).
12. V. V. Dobrovol'skii, "Geochemistry of trace elements in soil and biosphere," Pochvovedenie, No. 12, 68–78 (1984).
13. I. V. Zhurbin, A. V. Borisov, A. I. Nazmutdinova, V. N. Milich, R. P. Petrov, M. G. Ivanova, R. N. Modin, L. F. Knyazeva, N. G. Vorob'eva, and S. V. Zinchuk, "Complex use of remote survey, geophysics, and soil science methods in analysis of archeological monuments destroyed by soil tillage," Archaeol. Ethnol. Antropol. Eurasia, No. 2 (47), 103–111 (2019). https://doi.org/10.17746/1563-0102.2019.47.2.103-111
14. I. D. Zol'nikov, A. V. Postnov, V. A. Lyamina, V. S. Slavinskii, and D. A. Chupina, "GIS modeling of habitat conditions favorable for living of ancient man in Altai Mountains," Archaeol. Ethnol. Antropol. Eurasia, No. 3 (55), 40–47 (2013).
15. I. V. Ivanov, V. E. Prikhodko, I. V. Zamotaev, D. V. Manakhov, E. Yu. Novenko, P. I. Kalinin, L. M. Markova, and A.L. Plaksina, "Synlithogenic evolution of floodplain soils in valleys of small rivers in the Trans-Ural steppe," Eurasian Soil Sci. **52**, 593–609 (2019). https://doi.org/10.1134/S1064229319060061
16. V. B. Il'in, *Heavy Metals and Other Elements in the System Soil-Plant* (Siberian Branch, Russian Academy of Sciences, Novosibirsk, 2012) [in Russian].
17. A. Kabata-Pendias and H. Pendias, *Trace Elements in Soils and Plants* (CRC Press, Boca Raton, 1984; Mir, Moscow, 1989).
18. P. I. Kalinin, I. Yu. Kudrevatykh, I. M. Vagapov, A. V. Borisov, and A. O. Alekseev, "Biogeochemical processes in steppe landscapes of the Ergeni Upland in the Holocene," Eurasian Soil Sci. **51**, 495–505 (2018). https://doi.org/10.1134/S1064229318050058
19. N. S. Kasimov and D. V. Vlasov, "Clarks of chemical elements as the standards for comparison in ecogeochemistry," Vestn. Mosk. Univ., Ser. 5: Geogr., No. 2, 7–17 (2015).
20. V. S. Kurmanovskii, "Gnezdovo and its vicinities in 21st–18th centuries: historical-archeological complex," in *Gnezdovo Archeological Complex: Materials and Studies*, Tr. Gos. Istor. Muz. no. 1 (State Historical Museum, Moscow, 2018), pp. 241–266.
21. F. N. Lisetskii, T. N. Smekalova, and O. A. Marinina, "Biogeochemical features of fallow lands in the steppe zone," Contemp. Probl. Ecol. **9**, 366–375 (2016). https://doi.org/10.1134/S1995425516030094
22. F. N. Lisetskii, O. A. Marinina, and Zh. A. Buryak, *Geoarcheological Studies of Historical Landscapes of Crimea* (Voronezh, 2017) [in Russian]. www.researchgate.net/publication/322936359
23. S. P. Lomov, A. V. Lyganov, A. A. Khisyametdinova, I. N. Spiridonova, and N. N. Solodkov, "Modern and buried soils of kurgans in the forest-steppe zone of the Middle Volga region (by the example of Komintern I kurgan)," Eurasian Soil Sci. **50**, 539–548 (2017). https://doi.org/10.1134/S1064229317050106
24. M. V. Mikharevich, V. S. Myglan, and V. E. Prikhodko, "Reconstruction of Climate and Landscapes of the Medieval Ages on Basis of Paleosols Palinological Study and Dendrochronological Data of Altai (South of Western Siberia)", Eurasian Soil Sci. **53** No 5, (2020). (in press).
25. V. S. Myglan, O. Ch. Oidupaa, and E. A. Vaganov, "2367-year-long chronology of the Altai–Sayan region (Mongun–Taiga Massif) as based on tree rings," Archaeol. Ethnol. Antropol. Eurasia, No. 3, 76–83 (2012).

26. G. I. Nenasheva, *Vegetation and Climate of Intermontane Depressions of Central Altai in the Holocene* (Altai State Univ., Barnaul, 2013) [in Russian].
27. L. A. Orlova, *Holocene of Baraba* (Academy of Sciences of USSR, Novosibirsk, 1990) [in Russian].
28. T. V. Pampura, M. Meili, K. Holm, F. Candaudap, and A. Probst, "Buried paleosols as reference objects for assessing the current level of soil pollution with lead in the Lower Volga steppes," Eurasian Soil Sci. **52**, 34–49 (2019). https://doi.org/10.1134/S1064229319010113
29. A. A. Podgornaya, M. I. Dergacheva, and E. G. Zakharova, "Humus of paleosols of burial kurgan Sanatornyi-1 (Western Siberia) and reconstruction of pedogenesis conditions," Vestn. Tomsk. Gos. Univ., Ser. Biol., No. 328, 198–201 (2008).
30. N. V. Polos'mak and V. I. Molodin, "Monuments of Pazyryk culture on the Ukok Plateau," Archaeol. Ethnol. Antropol. Eurasia, No. 4, 66–87 (2000).
31. V. E. Prikhodko, I. V. Ivanov, D. G. Zdanovich, G. B. Zdanovich, D. V. Manakhov, and K. Inubushin, *Arkaim—Fortified Settlement of the Bronze Age of the Steppe Trans-Ural Region: Soil and Archaeological Research* (Moscow, 2014) [in Russian]. https://doi.org/10.13140/RG.2.1.3861.1369
32. V. E. Prikhodko, M. V. Mikharevich, Yu. A. Azarenko, M. R. Shayakhmetov, V. V. Gorbunov, A. A. Tishkin, and E. G. Pivovarova, "Interdisciplinary study of kurgans of Srostki-1 necropolis and climate reconstruction of ancient Altai region," in *Modern Solutions of Current Problems of Eurasian Archeology* (Altai State Univ., Barnaul, 2018), No. 2, pp. 119–123. file:///C:/Users/Prikhodko/Downloads/Современные_решения_актуальных_проблем_евразийской_археологии%20(1).pdf.
33. A. V. Puzanov and S. V. Baboshkina, "Arsenic in the soil-natural water-plant system of the Altai region," Eurasian Soil Sci. **42**, 996–1004 (2009).
34. N. E. Ryabogina, A. V. Borisov, S. I. Ivanov, O. G. Zanina, and N. M. Savitskii, "Environmental conditions in the south of Central Russian Upland in the Khazar time (9th–20th centuries)," Vestn. Arkheol., Antropol. Etnogr., No. 3 (22), 182–194 (2013).
35. O. A. Samonova, A. N. Gennadiev, T. S. Koshovskii, and A. P. Zhidkin, "Metals in the soils of a small watershed in the forest-steppe zone of the Central Russian upland," Eurasian Soil Sci. **48**, 584–592 (2015). https://doi.org/10.1134/S1064229315060101
36. N. F. Spitsyna, V. G. Bakharev, and G. G. Morkovkin, "Trace elements composition of chernozems in moderately dry and steep steppe of Altai krai," Vestn. Altai. Gos. Agrar. Univ., No. 11 (97), 43–45 (2012).
37. A. I. Syso, *The Distribution Patter of Chemical Elements in Pedogenic Minerals and Soils of Western Siberia* (Siberian Branch, Russian Academy of Sciences, Novosibirsk, 2007) [in Russian].
38. A. A. Tishkin, V. V. Gorbunov, and T. G. Gorbunova, *Altai in the Medieval Epoch: Illustrated Historical Atlas* (Barnaul, 2011) [in Russian].
39. Yu. G. Chendev, A. L. Aleksandrovskii, O. S. Khokhlova, M. I. Dergacheva, A. N. Petin, A. N. Golotvin, V. A. Sarapulkin, G. L. Zemtsov, and S. V. Uvarkin, "Evolution of forest pedogenesis in the south of the forest-steppe of the Central Russian Upland in the Late Holocene," Eurasian Soil Sci. **50**, 1–13 (2017). https://doi.org/10.1134/S1064229317010033
40. M. R. Shayakhmetov, V. E. Prikhodko, V. V. Gorbunov, and A. A. Tishkin, "Use of GIS and Earth remote survey data in the study of medieval Srostki culture in Altai krai," in *Proceedings of the V International Scientific Conference "Regional Problems of Remote Survey of the Earth," September 11–14, 2018* (Siberian State Univ., Krasnoyarsk, 2018), pp. 426–429.
41. A. R. Agatova, A. N. Nazarov, R. K. Nepop, and H. Rodnight, "Holocene glacier fluctuations and climate changes in the southeastern part of the Russian Altai (South Siberia) based on a radiocarbon chronology," Quat. Sci. Rev. **43**, 74–93 (2012). https://doi.org/10.1016/j.quascirev.2015.12.005
42. T. Blyakharchuk, A. Eirikh, E. Mitrofanova, H.-C. Li, and S.-C. Kang, "High resolution palaeoecological records for climatic and environmental changes during the last 1350 years from Manzherok Lake, western foothills of the Altai Mountains, Russia," Quat. Int. **447**, 59–74 (2017). https://doi.org/10.1016/j.quaint.2017.06.014
43. T. Blyakharchuk, V. Prikhodko, M. Kilunovskaya, and H.-C. Li, "Vegetation and climate reconstruction based on pollen records derived from burial mounds soil in Tyva Republic, Central Asia," Quat. Int. **507**, 108–123 (2019). https://doi.org/10.1016/j.quaint.2018.09.028
44. M.-L. Branvall, R. Bindler, I. Renberg, O. Emteryd, J. Bartniki, and K. Billstrom, "The medieval metal industry was the cradle of modern large-scale atmospheric lead pollution in northern Europe," Environ. Sci. Technol. **33**, 4391–4395 (1999).
45. M. Bronnikova, A. Panin, O. Uspenskaya, Yu. Fuzeina, and I. Turova, "Late Pleistocene-Holocene environmental changes in ultra-continental subarid permafrost affected landscapes of the Terekhol basin, South Siberia," Catena **112**, 99–111 (2014).
46. M. A. Bronnikova, Yu. V. Konoplyanikova, A. R. Agatova, M. P. Lebedeva, R. K. Nepop, and M. P. Lebedeva, "Holocene environmental change in south-east Altai evidenced by soil record," Geogr., Environ., Sustainability **11** (4), 100–111 (2018). https://doi.org/10.24057/2071-9388-2018-11-4-100-111
47. B. Buggle, B. Glaser, U. Hambach, N. Gerasimenko, and S. Marković, "An evaluation of geochemical weathering indices in loess–paleosol studies," Quat. Int. **240**, 12–21 (2011). https://doi.org/10.1016/j.quaint.2010.07.019
48. J. H. Chen, F. H. Chen, S. Feng, W. Huang, J. B. Liu, and A. F. Zhou, "Hydroclimatic changes in China and surroundings during the medieval climate anomaly and little ice age: spatial patterns and possible mechanisms," Quat. Sci. Rev. **107**, 98–111 (2015).
49. R. Cox, D. R. Lowe, and R. L. Cullers, "The influence of sediment recycling and basement composition on evolution of mudrock chemistry in southwestern United States," Geochim. Cosmochim. Acta **59**, 2919–2940 (1995).
50. P. N. Eze and M. E. Meadows, "Multi-proxy palaeosol evidence for late Quaternary (MIS 4) environmental and climate shifts on the coasts of South Africa," Quat. Int. **343**, 159–168 (2014).
51. T. M. Gallagher and N. D. Sheldon, "A new paleothermometer for forest paleosols and its implications for

Cenozoic climate," Geology **41**, 647–650 (2013). https://doi.org/10.1130/G34074.1

52. S. Gallet, B. Jahn, and M. Torii, "Geochemical characterization of the Luochuan loess-paleosol sequence, China, and paleoclimatic implications," Chem. Geol. **133**, 67–88 (1996).
53. A. Glebova and I. Sergeev, "Human settlement, landscapes and environmental change in the Russian Altai Mountains during the Holocene," Quat. Int. **470**, 176–193 (2018). https://doi.org/10.1016/j.quaint.2018.01.002
54. K. Goldberg and M. Humayun, "The applicability of the Chemical Index of Alteration as a paleoclimatic indicator: an example from the Permian of the Paraná Basin, Brazil," Palaeogeogr., Palaeoclimatol., Palaeoecol. **293** (1), 175–183 (2010). https://doi.org/10.1016/j.palaeo.2010.05.015
55. H. Herold, "Fortified settlements of the 9th and 10th centuries AD in central Europe: structure, function and symbolism," Medieval Archaeol. **56**, 60–84 (2012). https://doi.org/10.1179/0076609712Z.0000000003
56. Z. Hu and S. Gao, "Upper crustal abundances of trace elements: a revision and update," Chem. Geol. **253** (3–4), 205–221 (2008).
57. Z. Jacobs, B. Li, M. V. Shunkov, M. B. Kozlikin, N. S. Bolikhovskaya, A. K. Agadjanian, V. A. Uliyanov, S. K. Vasiliev, K. O'Gorman, A. P. Derevianko, and R. G. Roberts, "Timing of archaic hominin occupation of Denisova Cave in southern Siberia," Nature. **565**, 594–599 (2019). https://doi.org/10.1038/s41586-018-0843-2
58. A. Kabata-Pendias, *Trace Elements in Soils and Plants* (CRC Press, Boca Raton, 2011).
59. M. Klinge and D. Sauer, "Spatial pattern of Late Glacial and Holocene climatic and environmental development in Western Mongolia—A critical review and synthesis," Quat. Sci. Rev. **210**, 26–50 (2019). https://doi.org/10.1016/j.quascirev.2019.02.020
60. F. N. Lisetskii, V. F. Stolba, and V. I. Pichura, "Late-Holocene palaeoenvironments of Southern Crimea: soils, soil-climate relationship and human impact," Holocene **27** (12), 1859–1875 (2017). https://doi.org/10.1177/0959683617708448
61. G. Liu, L. Li, L. Wu, G. Wang, et al., "Determination of soil loss tolerance of an entisol in Southwest China," Soil Sci. Soc. Am. J. **73** (2), 412–417 (2009).
62. H. W. Nesbitt and G. M. Young, "Early Proterozoic climates and plate motions inferred from major element chemistry of lutites," Nature **299**, 715–717 (1982).
63. V. Prikhodko, T. Puzanova, T. Tregub, V. Berezutskiy, and F. Kurbanova, "Complex paleoecological research of buried soils and reconstruction of the Bronze age climate in the East European plain and adjacent area," in *Proceedings of the 18th International Multidisciplinary Scientific GeoConference SGEM 2018* (Albena, 2018), pp. 243–250. doi l.5593/sgem2018/5.2
64. S. Reinhold and D. C. Korobov, "The Kislovodsk basin in the North Caucasian piedmonts—archaeology and GIS studies in a mountain cultural landscape," Preistoria Alp. **42**, 181–207 (2007).
65. G. J. Retallack, "Soils and global change in the carbon cycle over geological time," in *Treatise on Geochemistry*, Vol. 5: *Surface and Ground Water, Weathering, and Soils* (Elsevier, Amsterdam, 2003), pp. 581–605.
66. N. Rudaya, L. Nazarova, D. Nourgaliev, O. Palagushkina, D. Papin, and L. Frolov, "Middle-late Holocene environmental history of Kulunda, southwestern Siberia, vegetation, climate and humans," Quat. Sci. Rev. **48**, 32–42 (2012). https://doi.org/10.1016/j.quascirev.2012.06.002
67. R. L. Rudnick and S. Gao, "Composition of the continental crust," in *Treatise on Geochemistry*, Vol. 3: *Crust* (Elsevier, Amsterdam, 2003), pp. 1–64.
68. B. Schilman, M. Bar-Matthews, A. Almogi-Labin, and B. Luz, "Global climate instability reflected by Eastern Mediterranean marine records during the late Holocene," Palaeogeogr., Palaeoclimatol., Palaeoecol. **176**, 157–176 (2001).
69. N. D. Sheldon and N. J. Tabor, "Quantitative paleoenvironmental and paleoclimatic reconstruction using paleosols," Earth-Sci. Rev. **95**, 1–52 (2009).
70. J. Skurzyński, Z. Jary, J. Raczyk, P. Moska, B. Korabiewski, K. Ryzner, and M. Krawczyk, "Geochemical characterization of the Late Pleistocene loess-palaeosol sequence in Tyszowce (Sokal Plateau-Ridge, SE Poland)," Quat. Int., (2018). https://doi.org/10.1016/j.quaint.2018.04.023
71. G. Taylor, C. F. Pain, and P. J. Ryan, "Geology, geomorphology and regolith," in *Guidelines for Surveying Soil and Land Resources* (Melbourne, 2008), pp. 45–60.
72. O. Tohru and A. Hiroyoshi, "Statistical empirical index of chemical weathering in igneous rocks: A new tool for evaluating the degree of weathering," Chem. Geol. **240**, 280–297 (2007). https://doi.org/10.1016/j.chemgeo.2007.02.017
73. J. N. J. Visser and G. M. Young, "Major element geochemistry and paleoclimatology of the Permo-Carboniferous glacigene Dwyka Formation and postglacial mudrocks in southern Africa," Palaeogeogr., Palaeoclimatol., Palaeoecol. **81**, 49–57 (1990).
74. K. H. Wedepohl, "The composition of the continental crust," Geochim. Cosmochim. Acta **59** (7), 1217–1232 (1995).
75. R. A. Wuana and F. E. Okieimen, "Heavy metals in contaminated soils: A review of sources, chemistry, risks and best available strategies for remediation," ISRN Ecol. **2011**, 40264 (2011). https://doi.org/10.5402/2011/402647
76. K. Ying, C. S. Frederiksen, X. Zheng, J. Lou, and T. Zhao, "Variability and predictability of decadal mean temperature and precipitation over China in the CCSM4 last millennium simulation," Clim. Dyn., (2018). https://doi.org/10.1007/s00382-017-4060-8
77. S. Zhilich, N. Rudaya, S. Krivonogov, L. Nazarova, and D. Pozdnyakov, "Environmental dynamics of the Baraba forest-steppe (Siberia) over the last 8000 years and their impact on the types of economic life of the population," Quat. Sci. Rev. **163**, 152–161 (2017).
78. D. Zhang and Z. Feng, "Holocene climate variations in the Altai Mountains and the surrounding areas: a synthesis of pollen records," Earth-Sci. Rev. **185**, 847–869 (2018). https://doi.org/10.1016/j.earscirev.2018.08.007

*Translated by D. Konyushkov*



SPELL: OK